

The first day or so, we all pointed to our countries. The third or fourth day, we were pointing to our continents. By the fifth day, we were aware of only one Earth.

Prince Sultan bin Salman bin Abdulaziz al Saud, Saudi Arabian astronaut (Sagan 1997, p. 139)

2.1 The Antarctic Ice Sheet

In German, an ice sheet of the type covering Antarctica is usually called an *Eisschild* or *Eispanzer*, which can loosely be translated as an “ice shield” or “ice armour”, respectively. While the English term “sheet” better describes the thin geometry of an ice sheet,¹ there is no doubt that the German names best convey the idea of a massive bulk of ice over Antarctica: with a volume of circa $25 \times 10^6 \text{ km}^3$ (including ice shelves) and an average thickness close to 2 km spread over an area larger than $13 \times 10^6 \text{ km}^2$, the Antarctic Ice Sheet contains about 23 million gigatonnes of ice, which represent roughly 67% of world’s freshwater and a potential contribution to global sea-level rise of 58 m (Lemke et al. 2007; Vaughan et al. 2013). As if these figures were not impressive enough, the Antarctic ice plateau is also the coldest desert in the world, with annual mean temperatures far below freezing and precipitation values comparable with the driest deserts on the globe.

As mighty as it may seem, the Antarctic Ice Sheet is not insensitive to external agents. Similar to other polycrystalline solids, ice yields in a ductile manner at sufficiently high temperatures, slowly flowing under the burden of its own weight in a highly viscous fluid-like regime of plastic deformation known as *creep*. As reference, metals and ceramics usually start to creep at temperatures above circa 30 and 50% of their

melting points, respectively (Frost and Ashby 1982; Phillips 2001). Thus, recalling that ice as cold as -40°C (which is a common temperature for Antarctic ice) is already at 85% of its melting point, it should come as no surprise that glaciers and ice sheets creep: this is an expected and unavoidable phenomenon, simply caused by the fact that the Earth’s surface is always considerably hot for ice.

This creep regime allows the ice in Antarctica to continually flow away over the centuries and millennia under the action of its own colossal weight, creeping towards the ocean at a pace from several to many metres per year (Bamber et al. 2000), until it eventually melts beneath ice shelves or calves into icebergs (Kirchner and Faria 2009; Kristensen 1983; Rignot et al. 2004). This ceaseless creep is mainly controlled by the ice temperature, and nourished by snowfall on its surface. As a consequence, climatic changes have a profound impact on the *mass balance* of the ice sheet, which is basically the difference between the gain through precipitation from the atmosphere (*snow accumulation*) and the loss through melting and calving to the ocean (*ice ablation*). If the balance is positive, the ice sheet grows, otherwise it dwindles.

The resulting climate-driven waxing and waning of the Antarctic Ice Sheet reflects its fundamental role in the Earth’s climate system, which is characterized by the ability of the ice sheet to interact with the atmosphere and the ocean on a global scale (Bamber et al. 2007; Hemming 2004; Oerlemans 2001; Siegert 2001). Evidences of these interactions can be easily found, e.g. in paleoclimate records showing the differences in the global climate before and after the emergence of large ice sheets in the early Oligocene (ca. 34 million years ago; Zachos et al. 2001), or in sea-floor sediments and paleoglacial landforms revealing massive ice discharges from ancient ice sheets (Bond et al. 1992; De Angelis and Kleman 2007).

Crucial is that such ice–environment interactions remain recorded also in the ice sheet itself. Within and together with the snow, further substances (aerosols, isotopes, etc.) are also deposited from the atmosphere onto the ice sheet surface. These deposits contain information about the atmospheric

¹The Antarctic Ice Sheet has a width-to-height aspect ratio of $\approx 1.8 \times 10^3$, which is of the same order of magnitude as the aspect ratio of a typical sheet of A4 office paper (cf. definition of *ice sheet* in Sect. 1.2).

composition in the period between the formation of snow crystals in the atmosphere, their precipitation and metamorphism into porous firn, and the subsequent transformation of firn into impermeable bubbly ice. The outcome of this metamorphic process is the chemical and structural stratification of polar ice, which can be observed in all ice cores retrieved from Antarctica (and Greenland). Many of these stratified impurities have already been identified as climate *proxies* (cf. Glossary in Sect. 1.2), which render the Antarctic ice sheet a unique archive of Earth's climate in the past million years (EPICA Community Members 2004; EPICA community members 2006; Petit et al. 1999; Watanabe et al. 2003).

At this point it is important to emphasize that the *active* interaction of the ice sheet with its environment (through its flow, albedo, melting, etc.) and its *passive* recording of the past climate are intimately coupled. For instance, experience shows that climate proxies in form of microscopic inclusions and dissolved impurities in polar ice can have a marked impact on the ice *microstructure* (see Glossary in Sect. 1.2), as exhibited e.g. in the conspicuous correlation between mean grain size of ice and impurity concentration within *cloudy bands* identified in polar ice cores (Faria et al. 2010, 2014a; Gow and Meese 2007a; Gow and Williamson 1976). On the other hand, as in any other polycrystalline material, the microstructure plays an essential role in defining the mechanical properties of ice, including its flow (also called *rheology*). From these facts we conclude that climate proxies not only build up the paleoclimate records of the ice sheet, but they also have a significant effect on the rheology of polar ice (Faria et al. 2009, 2014b; Gow and Meese 2007b; Lhomme et al. 2005; Paterson 1991, 1994).

It happens, however, that paleoclimate records are not always well preserved in polar ice. The main threat to record integrity is the ice flow, which generates considerable shearing in the lower part of the ice sheet. This shearing often causes disturbances and alterations in the ice strata (e.g. folds) that eventually lead to the disruption of the ice stratigraphy (Alley et al. 1997; Faria et al. 2010; NEEM Community Members 2013). Such disruptions render the interpretation of paleoclimate records in the deepest portion of ice cores (which is generally also the oldest and most valuable) a formidable task.

In summary, inclusions and dissolved impurities transferred from the atmosphere into the ice make up climate records that can have significant effects on the microstructure and rheology of polar ice. In turn, climate records stored within the ice are generally not static: the same ice that preserves paleoclimate records can also operate on them. The most serious operation is the disruption of the local stratigraphy by the ice flow. Fortunately, many of these operations leave temporary imprints on the ice structure, which can be identified and analysed through appropriate techniques. Some of these techniques are described in the next chapters. The identification of such temporary imprints allows glaciologists

to devise new methods for reconstructing disrupted climate records.

2.2 Understanding the SFEI

The interactions between impurities, microstructure, and mechanical properties of polar ice, outlined in the last section, are particular examples of a comprehensive multi-scale interpretation of the dynamics of natural systems called *Structure–Form–Environment Interplay (SFEI)* (cf. Fig. 2.1 and Glossary in Sect. 1.2). Generally, the term “structure” encompasses all constitutive features of the system that determine its symmetry and response on diverse scales. The notion of “form” is defined by the interior and boundaries of the system, so that changes in form include all morphological processes of deformation, flow, growth, decay, etc., undergone by the system. Finally, “environment” stands for all exterior circumstances and boundary conditions necessary to fully characterize the system in relation to its surroundings.

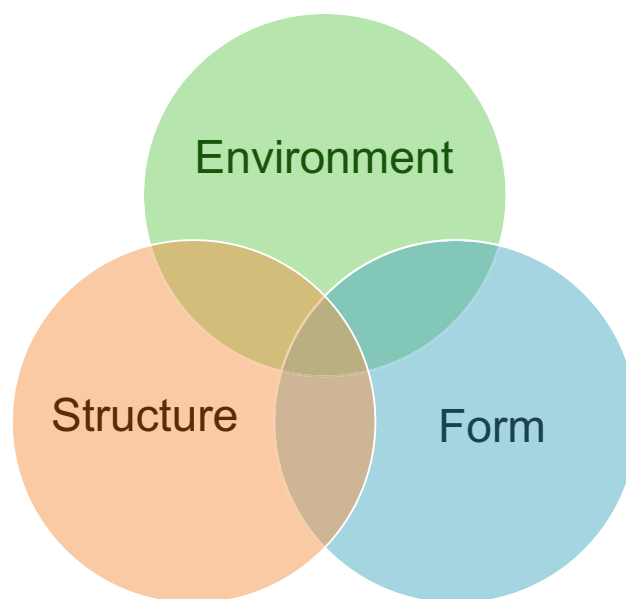


Fig. 2.1 Schematic representation of the Structure–Form–Environment Interplay (SFEI). The environment acts on form and structure; changes in form affect structure and environment; the structure influences form and environment

It must be emphasized that the general characterization of structure, form, and environment is far from resulting in a sharp trichotomy. In fact, these three concepts generally overlap considerably, so that their precise distinction depends largely on the context and the scale under consideration. For instance, in a large-scale ice-sheet model, the pore space of firn is part of the ice microstructure, while the atmosphere on the ice sheet belongs to the environment. In contrast, for a

glaciologist interested in the microscopic genesis of climate records, the pore space of firn defines the form, while the air inside the pores constitutes the environment.

For the sake of illustration, we may consider the notion of SFEI with regard to the problem of a large armada of *icebergs* drifting under the action of winds and ocean currents, as it occurs e.g. in the North Atlantic during *Heinrich events* or in the Southern Ocean during the collapse of Antarctic ice shelves:

- If the modeller is interested in the fate of a single iceberg, then the concept of *form* comprises the size and shape of that particular iceberg, while the ice crystallites, inclusions and impurities within the iceberg define its (micro- and macro-) *structure*. Accordingly, melting and fragmentation of the iceberg represent interactions between *form* and *environment*.
- A very different picture of SFEI emerges if the modeller is interested in the dispersion of the whole armada. In this case, the *form* consists of the spatial distribution (i.e. instantaneous positions) of all icebergs, while the sizes and shapes of individual icebergs define the (“micro-”) *structure* of the armada. Melting and fragmentation of icebergs represent now interactions between *structure* and *environment*.

The contextual flexibility in the definitions of structure, form, and environment within the SFEI are typical of complex systems with *nested* or *multiscale hierarchy*: the form of a small-scale system Σ becomes part of the structure of a larger system Λ , which is made up of many copies of the former (i.e. $\Sigma \subset \Lambda$). During this *upscaling* process, the definition of environment also changes, since form and environment are complementary concepts (the environment is exterior to the form).

To further explore the concept of SFEI within the context of Antarctica, we briefly review in the next section some of the typical structures observed in Antarctic ice, how they emerge, and how they interact with climate proxies and ice mechanical properties. Further details are discussed also in Chap. 4.

2.3 The Multiscale Structure of Antarctica

In the previous sections we introduced the notion of Antarctica as a *complex system*, with structural features on diverse scales, which evolves according to the framework of SFEI. Here we analyse this view in more detail, by investigating the formation and evolution of some key structural features of Antarctic ice: air inclusions.

Environmental conditions initially determine not only the size and shape of snow crystals (Fig. 2.2), but also the concentration of aerosols (mineral dust, sea salt, and other trace species) captured by the falling snow that accumulates on the

ice-sheet surface (McConnell et al. 2014; Fischer et al. 1998, 2007b). Stable isotope ratios of precipitation (HD^{16}O and H_2^{18}O relative to H_2^{16}O) are commonly used as proxies for the temperature at the time of snow formation, even though seasonal variations are usually lost by diffusive mixing (Cuffey and Steig 1998). Some types of snow crystals may be transported over long distances by strong winds, eventually accumulating selectively in a variety of surface patterns on multiple size scales, ranging from millimetre-thick wind crusts, to snowdrifts and sastrugi, up to vast megadunes (Birnbaum et al. 2010; Frezzotti et al. 2002; cf. Glossary in Sect. 1.2). These multiscale surface structures are then further modified by wind erosion, sublimation, and the rapid metamorphism of snow, triggered by direct exposition to solar radiation, wind, moisture, and temperature gradients (Colbeck 1983; Davis et al. 1996).

The surface of the Antarctic Ice Sheet essentially consists of such patches of multiscale surface structures made up of different types of compacted and eroded snow, which have been discontinuously formed during snowfall and wind events over several years (Fig. 2.3). The diverse granular compositions found in these multiscale surface structures are characterized by contrasts in grain size and shape, lattice preferred orientations, porosity, impurity and moisture content, which have their origins in intricate chemical and metamorphic processes in the snowpack. Air–snow exchanges of trace compounds affect the chemistry of the snow cover and the lower atmosphere, therefore interfering with the snow metamorphism (Dominé and Shepson 2002; Grannas et al. 2007). Besides the evident consequences for the formation of climate proxies, changes in snow chemistry and metamorphism can alter the surface albedo and permeability of the snow cover, with implications for the validation of radar backscatter signals from altimetry/interferometry surveys (RADARSAT, CryoSat, etc.; West et al. 1996).

Subsequent compaction and sintering of the old snow, driven by the increasing overburden of new snowfalls, leads to the formation with depth of the porous material known as *firn* (Figs. 2.4 and 2.5). In dry polar regions, the firn layer extends from the near surface² down to 50–100 m depth, with a gradual mass density increase (called *firn metamorphism/densification*, or *firnification*) from about 300–350 kg/m³ to 840 kg/m³, the latter defining the transition from

²It must be warned that the definition of firn presented in the Glossary (Sect. 1.2) requires some care, when applied to the dry, cold, and windy Antarctic plateau. As illustrated in Fig. 2.3, snow accumulation on this region is so low that its snow cover is discontinuous. That is, the plateau’s surface is generally characterized by a patchy coexistence of shallow snowdrifts and sastrugi with firn-exposed regions that may experience mass loss (ablation) through wind erosion and sublimation for several years. Consequently, firn with distinct physical properties (e.g. mass density, crystalline and pore structures, mechanical strength, etc.) can be found in neighbouring patches near the surface, making the distinction among old snow and various types of firn not so straightforward.

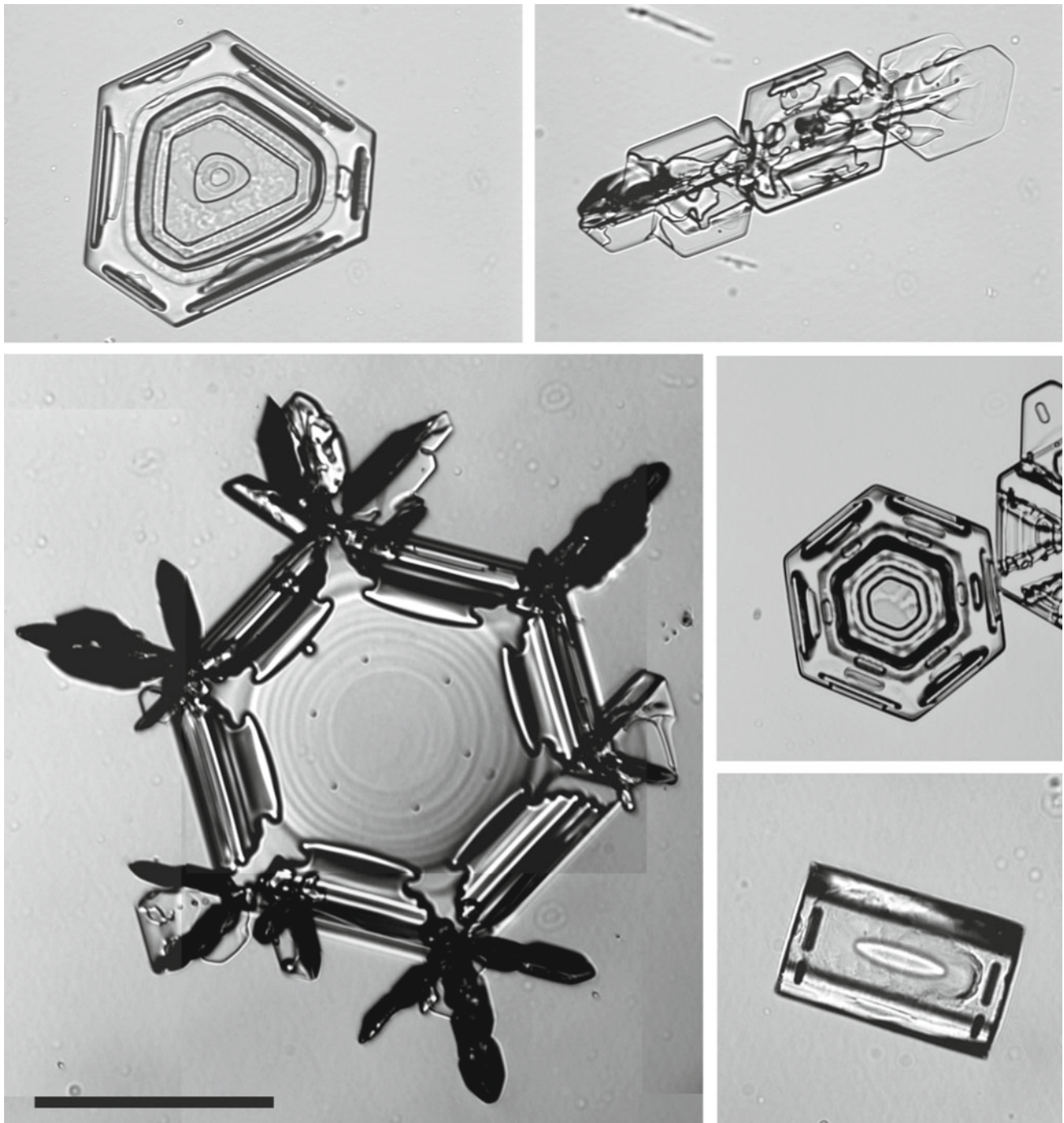


Fig. 2.2 Typical snow crystals at Kohnen Station, Dronning Maud Land, Antarctica. Fresh snow that falls on the cold and dry Antarctic plateau is usually monocrystalline (therefore the term *snow crystal*). In contrast, fresh snowflakes (viz. feathery aggregations of snow crystals typical of snowfalls in mid-latitudes) are rare. Nevertheless, snow crystals already deposited on the surface may sometimes aggregate into flakes, being eventually blown by strong winds up to considerable heights and distances. Scale bar: 1 mm

firn to *bubbly ice*. In the first 10–20 m below surface, seasonal temperature variations can penetrate into the firn and air exchange with the outer atmosphere occurs mainly through forced convection, in response to pressure gradients at the surface (Alley et al. 1982; Bender et al. 1994; Colbeck 1989).

Deeper down, gas transport occurs predominantly via diffusion driven by water-vapour density gradients (Colbeck 1983).

Evidently, the air exchange and transport within the firn is strongly constrained by the geometrical and topological



Fig. 2.3 Typical “patchwork” of multiscale surface structures on the Antarctic Ice Sheet. It consists of various types of snow covers with height variations not larger than many centimetres: flat-fissured (*bottom-right*), crinkly (*bottom and centre-left*), loosely rough (*centre*), and wavy-stepped (*centre-right*). Each of these covers is characterized by certain grain and pore microstructures, and has been produced by a particular combination of snow deposition, drift, sublimation, and erosion processes. The predominant wind direction in this site is from the *bottom-right* to the *top-left*. Image width corresponds approximately to 3 m at the bottom of the photograph

characteristics of the pore space, which in turn depend on the original structure of the snow cover and the whole history of firn metamorphism. Owing to this, a great variety of firn densification models have been proposed in the literature (e.g. Alley 1987; Herron and Langway 1980; Maeno and Ebinuma 1983; Barnola et al. 1991; Salamatin et al. 2009; Arnaud et al. 2000; Arthern et al. 2010; Freitag et al. 2013; Goujon et al. 2003). Common to all these models is the observance of two sintering stages, described by Anderson and Benson (1963) in terms of the mass density of firn ρ_f as follows (the critical densities mentioned below are just approximate, since they actually depend on several factors, like temperature or impurity content of the firn layer, as discussed by Arnaud et al. 2000):

1. *Snow and shallow-firn metamorphism* ($\rho_f < 550 \text{ kg/m}^3$). Densification is controlled by the structural rearrangement of unbounded snow and bounded firn particles by mechanical packing and grain-boundary sliding. The first critical density ($\approx 550 \text{ kg/m}^3$) corresponds to the limit beyond which grain-boundary sliding is no longer effective as the

controlling densification process, giving place to intracrystalline plastic deformation (creep).

2. *Deep firn metamorphism* ($550 \text{ kg/m}^3 \leq \rho_f < 820\text{--}840 \text{ kg/m}^3$). Firnification is controlled by intracrystalline power-law creep and recrystallization. The last critical density ($\approx 820\text{--}840 \text{ kg/m}^3$) defines the *pore close-off depth interval*, also called *firn–ice transition zone*, in which intercommunicating pores are pinched off and the air becomes entrapped in independent bubbles within the newly formed bubbly ice.

In addition to these two stages, Maeno and Ebinuma (1983) identified another critical density ($\approx 730 \text{ kg/m}^3$), which divides the second stage into two sub-stages. Although this critical density could be identified in the firnification curves of several firn cores, its physical grounds (proposed by Maeno and Ebinuma 1983, in terms of topological changes in the pore space) remained obscure for long time. This issue has been recently revisited by Kipfstuhl et al. (2009) and Faria et al. (2014b), who proved through observations and theory that the Maeno–Ebinuma critical density is actually

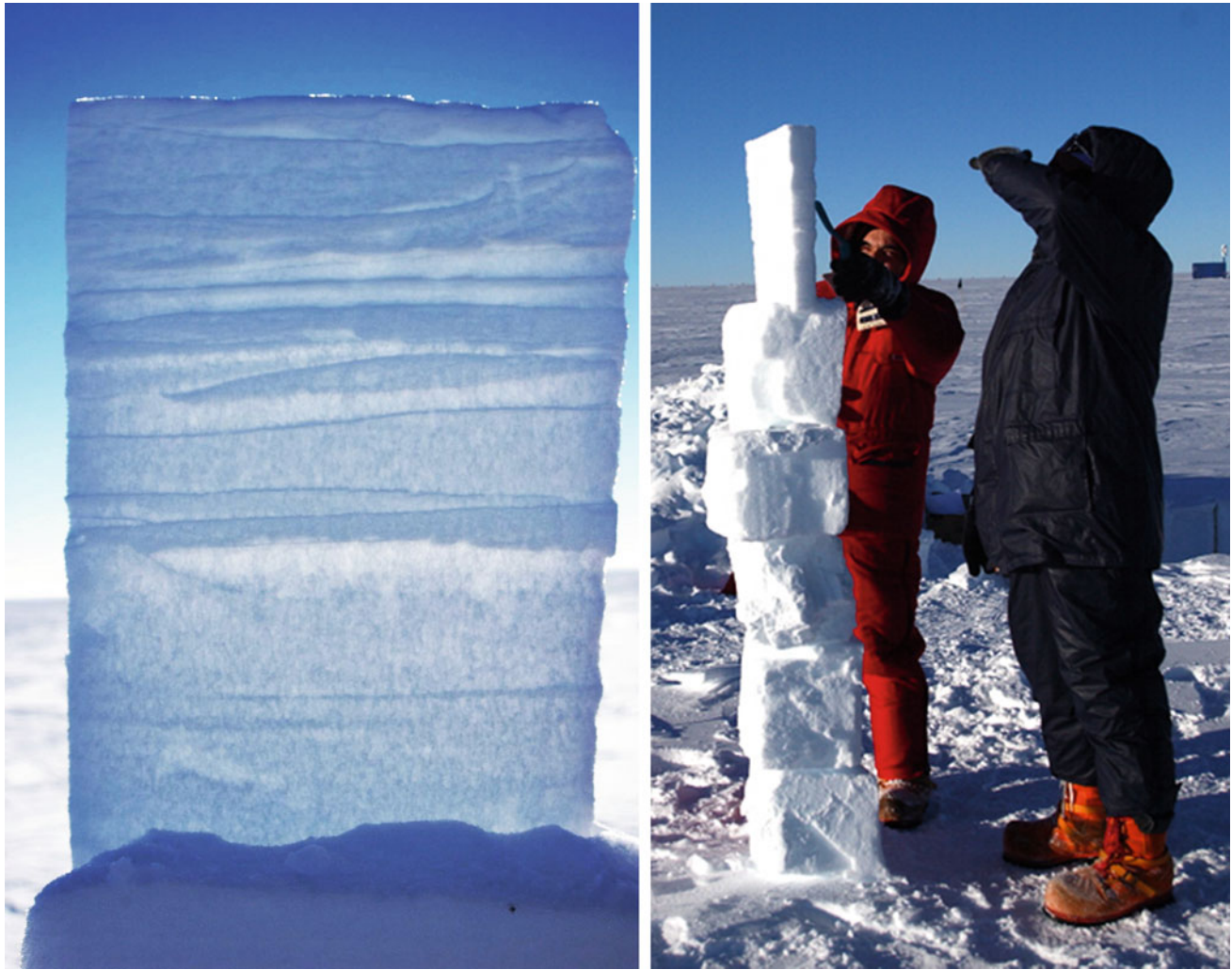


Fig. 2.4 The birth of Antarctic firn. *Left:* In a sense, this tablet may be regarded as the “Rosetta stone” of polar glaciology. It displays the uppermost 50 cm of firn (corresponding to several years of accumulation at DML), and reveals the genesis of the polar ice microstructure. Over the years, recurrent burial of diverse types of surface structures gives rise to a vertical sequence of fine- and coarse-pored strata, which are easily identified on the tablet when it is observed against sunlight. Each stratum has its own characteristic microstructure, impurity content, etc. Notice how the irregular structures at the top become gradually more compacted and regular with depth. *Right:* Set-up used for observing the tablet shown on the left. Firn blocks extracted from a nearby snow pit are piled together and used as a support for the tablet. Erosion and sublimation (intensified by exposing of the tablet to wind and sunlight) enhance the microstructural contrasts

caused not only by topological changes in the pore space, but mainly by changes in the crystalline structure and mechanical properties of the firn skeleton:

- 2.a. *Upper (deep) firn metamorphism* ($550 \text{ kg/m}^3 \leq \rho_f < 730 \text{ kg/m}^3$). Densification is controlled by intracrystalline power-law creep with strain hardening, characterised by the development of many regions with high internal stresses. The topology of the pore space reaches a state where its contribution to strain accommodation becomes negligible.
- 2.b. *Lower (deep) firn metamorphism* ($730 \text{ kg/m}^3 \leq \rho_f < 820\text{--}840 \text{ kg/m}^3$). Internal stress concentrations become so high that the stored strain energy in many regions

reaches the critical level to trigger dynamic recrystallization (SIBM-O and SIBM-N, cf. Sect. 1.2), causing strain softening and redistribution of internal stresses.

At the critical depth for pore close-off (named *firn–ice transition zone*), firn converts into bubbly ice, and the formerly connected pore space splits into many separated air bubbles, which take up approximately 10% of the total volume of bubbly ice (Stauffer et al. 1985). These air bubbles represent a *unique climate archive* for the reconstruction of past changes in atmospheric composition. Owing to the above-mentioned exchange and transport of air within the firn, however, the precise dating of these air bubbles (also known as the *ice–air age difference*) turns out to be a challenging task: gas inclusions

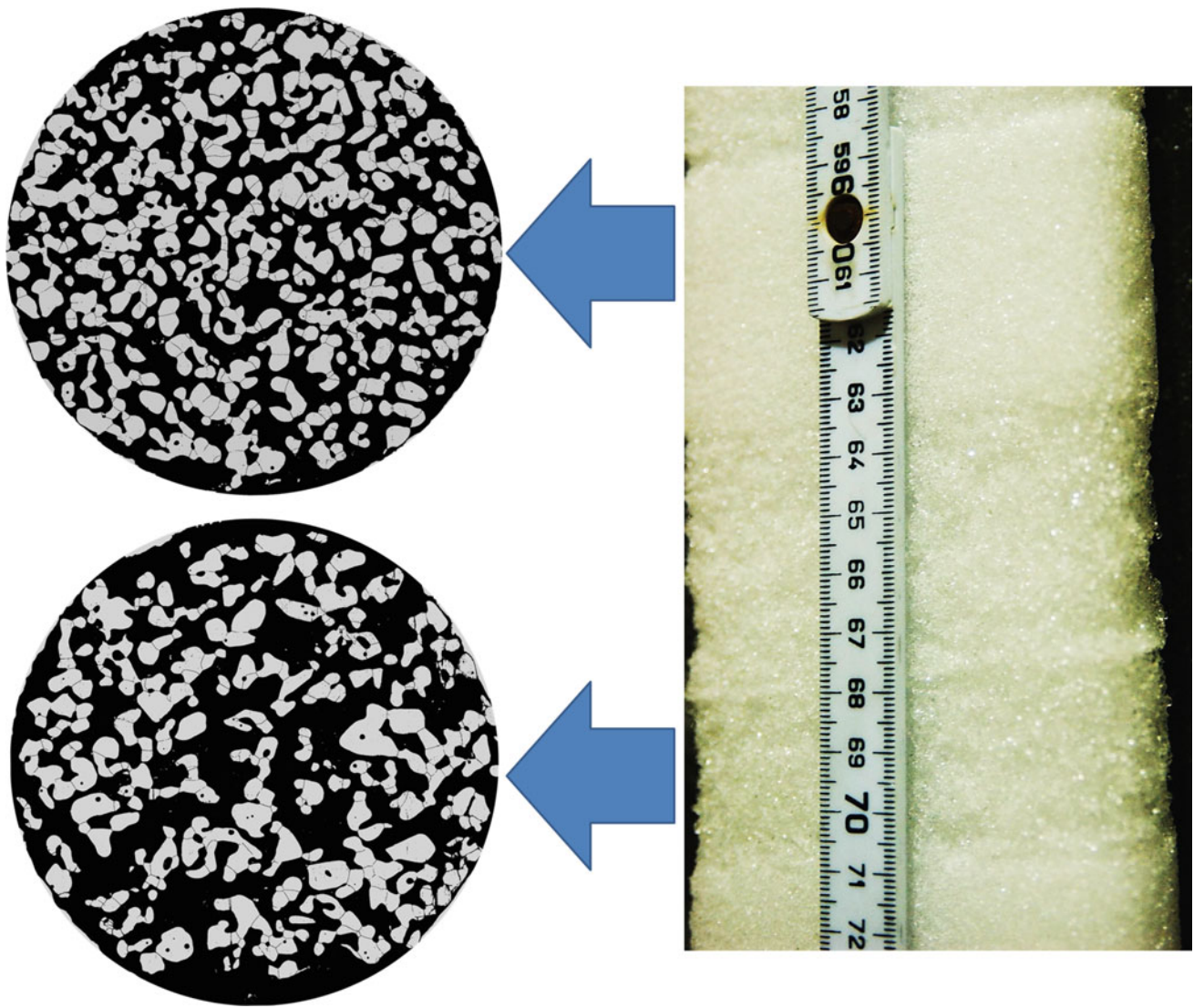


Fig. 2.5 Multiscale structure of an Antarctic firn sample from some metres depth (EDML B36 firn core). *Right*: Millimetre-thick wind crust (near the 68 mark) sandwiched between coarse-pored material, which is in turn surrounded by fine-pored firn. *Left*: Photomicrographs of horizontal sections showing the microstructures of the coarse- and fine-pored strata. The pore space appears in *black* and the ice skeleton in *light grey*. Some grain boundaries (faint dark lines inside the ice skeleton) can also be identified. The diameter of each micrograph is ca. 35 mm. In spite of the profound microstructural changes caused in firn by recrystallization and metamorphism, essential microstructural contrasts remain recorded in deeper ice (Bendel et al. 2013; Ueltzhöffer et al. 2010) as variations in the mean grain size, as well as in the number, average size, and spatial distribution of air bubbles

are always younger than the surrounding ice matrix. Air in firn pores down to 50–100 m depth still is in exchange with the atmosphere through connected pathways in the pore network. As a consequence, ice underneath the firn–ice transition depth can be a few thousand years older than the air entrapped in its bubbles (Barnola et al. 1987; Bender 2002; Raynaud et al. 2007; Schwander and Stauffer 1984).

The main source of complication comes from the fact that the firn mass density shows strong stratification, so that the resulting depth-variations in the pore structure entail critical differences in the exchange and transport of air between adjacent layers. High-resolution density studies of Arctic and

Antarctic firn (Gerland et al. 1999; Hori et al. 1999; Freitag et al. 2004; Hörhold et al. 2011, 2012) revealed that the initially strong density stratification (viz. *density variability*) caused by irregular snow deposition (Figs. 2.4 and 2.5) rapidly decreases within the shallow firn. Notwithstanding, the density variability increases again below 10–30 m depth, where the firn reaches a density of ca. 600–650 kg/m³, and it continues to increase, correlating with the impurity content, down to the firn–ice transition. Finally, in the bubbly ice zone, the density variability slowly diminishes again. These results suggest that density variations at the firn–ice transition, which are crucial for the dating of air bubbles, may be mainly caused by

variations in impurity content (Hörhold et al. 2012; Freitag et al. 2013).

Besides, recent studies by Ueltzhöffer et al. (2010) and Bendel et al. (2013) have shown that the *collective bubble structure* of bubbly ice (i.e. statistical data on bubble sizes, shapes, and spatial distribution) can be used to reconstruct the primordial pore structure of firn (viz. the *firn paleo-pore structure*). Such reconstructions tell us that layers with high impurity concentration, which are most frequent in glacial periods, reach the critical density for pore close-off first, therefore diminishing the ice–air age difference in ice from glacial periods.

In summary, a correct interpretation of climate records in the upper part of polar ice cores depends on identifying the links between atmospheric composition and the climate signal stored in the ice, together with a reliable dating of the ice matrix and its inclusions (Legrand and Mayewski 1997). Both issues are strongly connected to the structural properties of snow and firn, as well as their accumulation rate and metamorphism. As if the above arguments were not enough to underline the importance of structural studies of snow and firn, it has been recently recognized (Cuffey 2008; Helsen et al. 2008) that variations in the rate of firn metamorphism and snow accumulation over years and decades complicate assessments of Antarctic mass changes based on altimetry surveys, to such an extent that they represent today the main source of uncertainty in predictions of future sea level rise.

Beneath the firn–ice transition, air bubbles gradually decrease in size and the enclosed gas pressure increases with depth, in order to counterbalance the overburden pressure of ice (Bendel et al. 2013; Lipenkov et al. 1997; Salamatin et al. 1997, 2009; Ueltzhöffer et al. 2010). This increase of gas pressure with depth does not proceed indefinitely, though. Below a certain critical depth (which depends mainly on the pressure and temperature of the ice matrix), the ice–bubble composite structure is no longer thermodynamically stable, so that the gas and water molecules rearrange themselves into crystalline compounds called *clathrate hydrates* (cf. Glossary in Sect. 1.2; Shoji and Langway, Jr. 1982; Kipfstuhl et al. 2001; Salamatin et al. 2001). Clathrate hydrates in polar ice are composed of air, therefore being frequently called *air hydrates*.

The bubble–hydrate conversion in ice sheets is an intriguing microstructural phenomenon, which remains poorly understood. Air hydrates in polar ice seem to refuse complying with the simple thermodynamic theory that successfully explains hydrate formation in other environments, like pipelines or the sea floor (Miller 1969; Sloan 1998): not all bubbles in polar ice transform into air hydrates at the same critical depth predicted by the simple theory (which corresponds to the depth at which the overburden pressure of ice equals the theoretical clathrate–hydrate dissociation pressure, cf. Glossary in Sect. 1.2). Rather, there exists a large

depth interval that comprises the *bubble–hydrate transition zone*, which generally spans circa 500 m (corresponding to thousands of years), where bubbles and hydrates coexist (Fig. 2.6; Faria et al. 2010, 2009; Kipfstuhl et al. 2001; Narita et al. 1999; Pauer et al. 1996; Shoji and Langway, Jr. 1982, 1987; Uchida et al. 1994a, 2014).

Within this zone, which in the case of EDML covers the 800–1200 m depth interval (Faria et al. 2010, 2009), some interesting physical and chemical phenomena take place. In particular, there occurs a depth-dependent gas fractionation, with N₂-enriched bubbles co-existing with O₂-enriched hydrates (Ikeda et al. 1999; Nakahara et al. 1988). This fractionation is significant, with N₂/O₂ concentration ratios within clathrate hydrates reaching values around 2 or less at the upper part of the bubble–hydrate transition zone. Deeper down, this ratio gradually increases with depth again, moving back to the standard average atmospheric ratio of 3.7, which is achieved underneath the transition zone and coincides with the N₂/O₂ ratio originally found in the air bubbles above this zone. A similar fractionation phenomenon is observed also in the case of carbon dioxide (Stauffer and Tschumi 2000), with air hydrates at the upper part of the bubble–hydrate transition zone being depleted of CO₂.

The current explanation for this local air fractionation phenomenon lies in a combination of the lower hydrate dissociation pressure of O₂ and its ability to diffuse through ice faster than other air components, like N₂ or CO₂ (Ikeda-Fukazawa et al. 2005, 2001; Nedelcu et al. 2009; Severinghaus and Battle 2006; Stauffer and Tschumi 2000). Thus, the air diffusion from bubbles to hydrates through the ice matrix, caused by the higher pressure in the bubbles compared to the hydrate dissociation pressure, turns out to be more effective for O₂ than for N₂ or CO₂.

From the viewpoint of ice-core paleoclimate records, the phenomenon of bubble–hydrate air fractionation may cause serious complications for small-scale, high-resolution studies. Such studies are crucial for identifying abrupt variations in the past composition of Earth's atmosphere, and are especially important for the study of deep ice records, where the stratigraphy has already thinned considerably due to the ice-sheet flow. It has also been recognized that small changes in the N₂/O₂ ratio (in the per-mil range) correlate well with the local summertime insolation and could, in theory, be used as an absolute dating tool for ice cores (Bender 2002; Fujita et al. 2009; Suwa and Bender 2008). In both cases, the gas diffusion associated with air fractionation in the bubble–hydrate transition zone has the potential to spoil the integrity of high-resolution paleoclimate records.

The complications caused by air fractionation are however not limited to the bubble–hydrate transition zone: air hydrates in deep ice cores extracted and stored at atmospheric pressure are no longer in thermodynamic equilibrium, and therefore they tend to slowly dissociate air back into bubbles

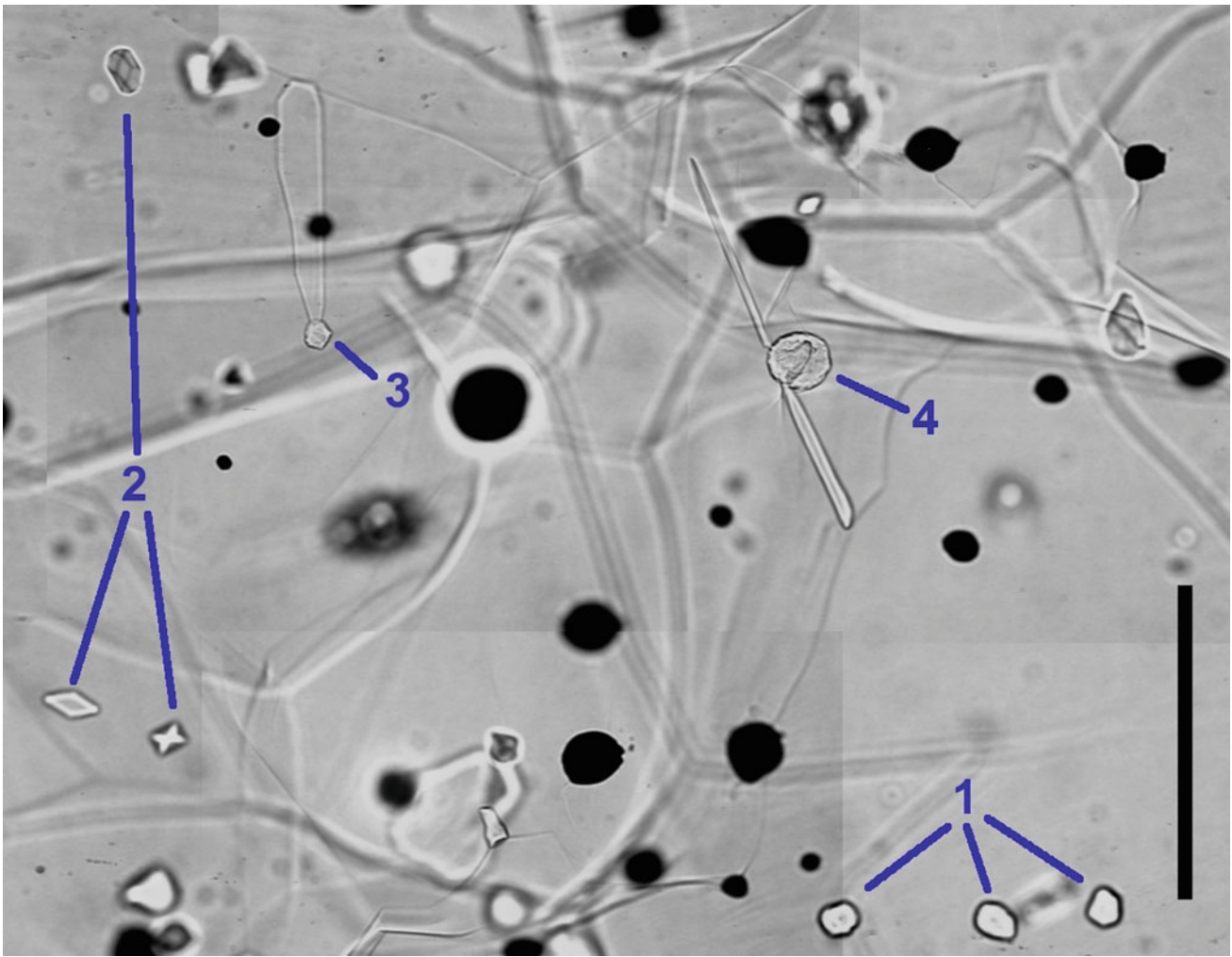


Fig. 2.6 Mosaic micrograph of the interior of a fresh EDML deep ice-core sample from 1055 m depth. It shows air bubbles and hydrates coexisting within the bubble–hydrate transition zone. Air bubbles appear *dark* and round, while air hydrates seem translucent. Defocused lines crossing the image in various directions are by-products of sample preparation, viz. grain-boundary marks (sublimation grooves) etched on both surfaces of the ice sample. Four types of air hydrates are explicitly identified: (1) rugged spheroids; (2) polyhedral shapes; (3) rugged spheroid with a large multifaceted protrusion; (4) rugged spheroid with two slender prolongations. The sample is “fresh” in the sense that it was prepared and analysed shortly after drilling, in order to minimize the effects of post-drilling relaxation (plate-like inclusions, secondary microbubbles, decomposing hydrates, etc.). Vertical scale bar: 1 mm

(Gow and Williamson 1975; Stauffer and Tschumi 2000). The rate of hydrate dissociation is mainly determined by the storage temperature (under atmospheric pressure) and may take between few and many years. This means that the coexistence of bubbles with hydrates in stored ice cores is inevitable, and consequently so are also the local diffusion and fractionation of air components, which can be minimized, but not fully avoided, by low temperature storage (Miyamoto et al. 2009; Gow 1971; Uchida et al. 1994b). For these and other reasons, a clear understanding of the interplay between ice microstructure and climate proxies is essential for the correct interpretation of high-resolution paleoclimate records.

Below the bubble–hydrate transition zone, air hydrates continue to evolve over millennia in curious ways (Fig. 2.6):

from rugged polycrystalline spheroids to multifaceted, polyhedral, and slender shapes, as well as smooth single-crystalline globules (Kipfstuhl et al. 2001; Pauer et al. 1999; Shoji and Langway, Jr. 1982; Uchida et al. 1994a). The causes of these varied recrystallization and metamorphic processes remain unclear.

Studies of climate records in the lowest tens of metres of deep ice cores are usually impaired by stratigraphic disturbances (e.g. folds) and interactions with subglacial encroachments (e.g. soil particles, rock fragments, melt water, etc.). Additionally, regardless of careful storage at low temperatures (usually between -20 and -50 °C), post-drilling relaxation structures emerge quickly and unavoidably in deep ice cores. They consist mostly of the previously mentioned

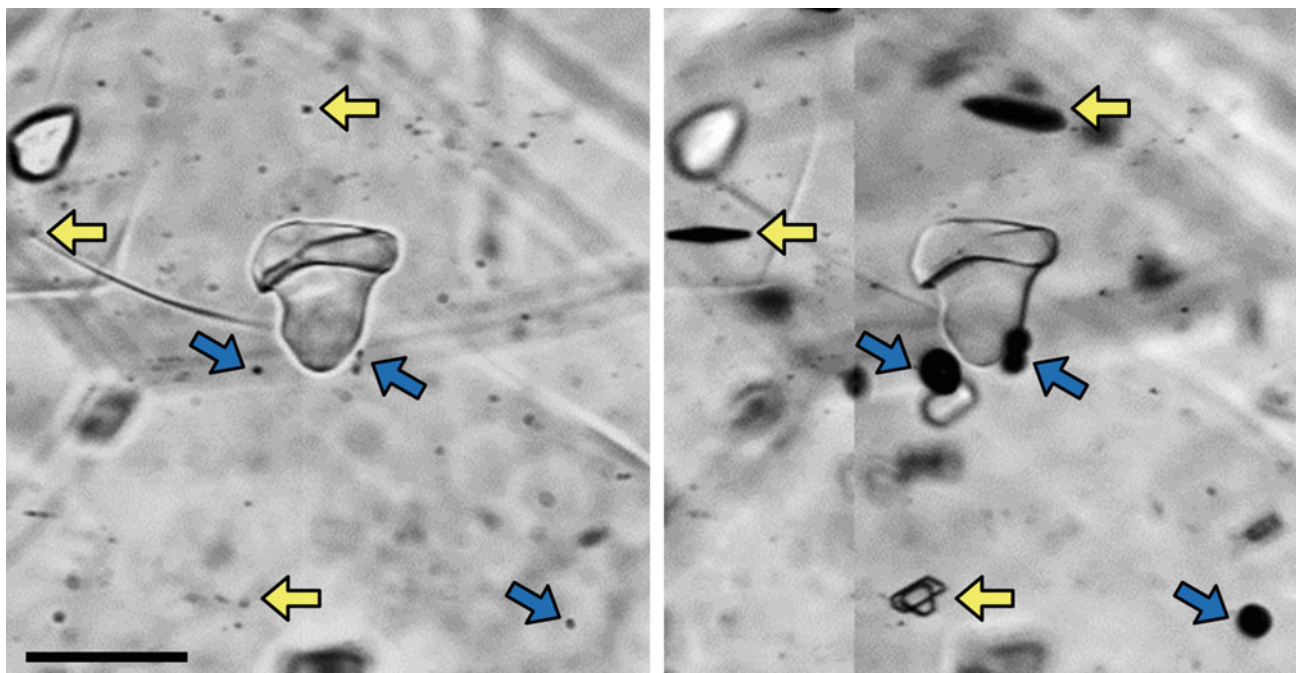


Fig. 2.7 Examples of post-drilling relaxation microstructures. *Left*: Fresh EDML ice core sample from 1095 m depth. Noticeable are a large hydrate in the centre and another smaller one at the *top-left* part of the image. The many *black dots* are microinclusions characteristic of cloudy-band ice (see Glossary in Sect. 1.2). *Right*: The same sample after three years of relaxation under standard storage conditions (-30°C and atmospheric pressure). At the locations of some microinclusions, secondary microbubbles (inclined *dark-blue arrows*) or plate-like inclusions (*horizontal light-yellow arrows*) have appeared. Interestingly, other microinclusions seem unaltered and show no signs of relaxation, possibly due to distinct physico-chemical properties. Scale bar: $100\mu\text{m}$. After Weikusat et al. (2012)

decomposing hydrates, microscopic relaxation bubbles called *secondary microbubbles*, and flat hexagonal cavities (i.e. negative crystals) known as *plate-like inclusions* (PLIs); cf. Fig. 2.7 and Glossary in Sect. 1.2 (Gow 1971; Nedelcu et al. 2009; Weikusat et al. 2012). Secondary microbubbles and PLIs are generally filled with fractionated (oxygen-enriched) air that was originally dissolved in the ice matrix or stored in air bubbles and hydrates. The characteristic O_2 enrichment of these relaxation structures suggests that the gas filling process occurs via molecular diffusion through the ice matrix, in a similar fashion as the filling of new air hydrates in the bubble-hydrate transition zone. Consequently, studies of PLIs and secondary microbubbles may help to clarify the mechanisms of gas diffusion in polar ice, in particular those related to air fractionation and metamorphism of air hydrates.

2.4 The Birth of EPICA

In a certain sense, one may say that the origins of the European Project for Ice Coring in Antarctica (EPICA) can be traced back to the end of 19th century, when Carl Weyprecht (1838–1881) developed the concept of “International Polar Year” (IPY). The basic purpose of IPY was to convince scien-

tists and policy makers that a coordinated international effort was needed to investigate the geophysics of polar regions. Weyprecht did not live to see his idea materialized: the *First International Polar Year* occurred in the period 1882–1883, shortly after his death. It became a milestone of polar glaciology, with twelve participating nations coordinated by an International Polar Commission, chaired by Georg von Neumayer (1826–1909). Besides many scientific advances and the completion of 15 polar expeditions (including two to Antarctica), the principal legacy of the First IPY was to set a precedent for international cooperation in science.

The example of international cooperation given by the First IPY inspired many subsequent scientific events and activities, including the *Second International Polar Year*, half century later (1932–1933). World War II imposed a hiatus in non-military polar research, but international research activities resumed shortly afterwards, following the spirit established by the first two IPYs. In particular, close scientific collaboration between Norway, Sweden, and Great Britain, initiated by Hans Ahlmann (1889–1974), culminated with the 1949–1952 *Norwegian–British–Swedish Antarctic Expedition* (NBSAE) led by John Giæver, Valter Schytt, and Gordon Robin (Schytt 1974), which recovered a nearly 100 m deep ice core from the *Maudheim* site on Quar Ice Shelf, Dronning Maud Land (DML), Antarctica (Faria et al. 2014a; Schytt

1958). NBSAE became a landmark in the history of geosciences not only because it provided *the very first Antarctic ice core* and launched the investigations of Antarctica's multiscale structure, but also because it established many aspects of the paradigm of scientific research to be pursued during the succeeding International Polar Year, which was expanded and renamed the *International Geophysical Year* (IGY, 1957–1958).

One of the main goals of IGY was to redirect the technology developed during World War II towards applications to geophysical research. Among the many scientific advances associated with this event, one could mention the verification of Alfred Wegener's theory of continental drift, the launching of the first artificial satellites (Sputnik series, Explorer series, Vanguard), and the discovery of the Van Allen radiation belt. Additionally, it established an international research cooperation programme in Antarctic glaciology of unprecedented proportions: 12 nations, 48 Antarctic stations, and diverse traverses over the Antarctic ice sheet, which provided not only the first informed estimates of Antarctica's total ice volume, but also two intermediate-depth ice cores extracted from *Byrd Station* (1957–1958, 307 m deep) and *Little America V* (1958–1959, 264 m deep; Langway 2008). Finally, another historical outcome from this period was the preparation of the *Main Antarctic Treaty*, ratified in 1961 by the twelve countries active in Antarctica during the IGY. Today, this Treaty still plays a fundamental role in preserving the environment and regulating human activity in Antarctica.

After the IGY in the late 1950s, a new era of polar glaciology was established, marked by the quest for ever deeper and older polar ice cores. In this vein, two prominent U.S. Army scientists, Henri Bader (a key person behind the IGY ice-core drilling campaigns) and his colleague B. Lyle Hansen (a world-renowned ice-core driller) started devising a plan to reach bedrock depths in Greenland and Antarctica (Bader 1962). In 1966, after a strenuous six-year field effort, the *first deep ice core reaching bedrock* (1387 m depth) was extracted from *Camp Century*, Northwest Greenland, a subterranean nuclear-powered overwintering facility for 200 persons operated by the U.S. Army (Ueda and Garfield 1968).

Surprisingly, in a genuine tour de force the same team and equipment continued their lucky streak by reaching bedrock in Antarctica less than two field seasons later, with the extraction of a 2164 m deep ice core from *Byrd Station* in 1968 (Ueda and Garfield 1969).

Whereas U.S. scientists primarily performed the aforementioned drilling operations, the ice-core laboratory analyses demanded an internationally coordinated action, mainly involving Denmark, Switzerland, and the United States. This collaboration culminated with the creation of the American–Danish–Swiss drilling initiative GISP (*Greenland Ice Sheet Project*), headed by Willi Dansgaard (University of Copenhagen), Chester Langway, Jr. (U.S. Army Polar

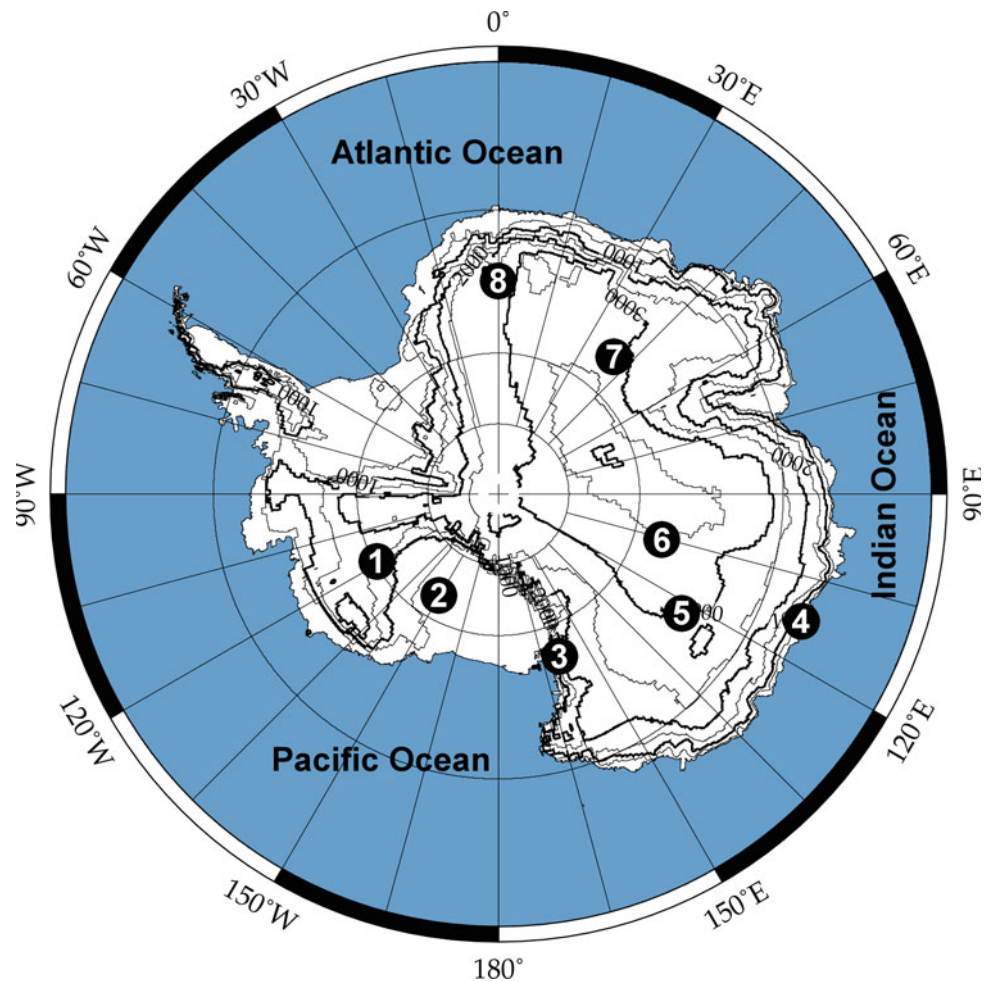
Research Unit), and Hans Oeschger (University of Bern). Three bedrock core drillings were originally planned for GISP, the major one at Summit, the highest point of the Greenland ice sheet. However, financial restrictions from U.S. side forced the selection of only one location, the logistically more convenient *Dye-3* site, a U.S. radar station near Greenland's southern coast. By 1981 bedrock was reached at Dye-3, yielding a 2037 m deep ice core.

The experience acquired with GISP, combined with the prevalent trend towards a unified European community (including the establishment of the *European Science Foundation*, ESF, in 1974) motivated European scientists to pursue joint inter-European deep drilling initiatives. The first of them, called GRIP (*Greenland Ice Core Project*), was coordinated by a steering committee chaired by Bernhard Stauffer (University of Bern) and involved eight European countries (Denmark, Switzerland, France, Germany, United Kingdom, Italy, Iceland and Belgium). Its aim was to drill an ice core down to Greenland's bedrock at Summit (the same drilling site originally planned for GISP). Simultaneously, a companion U.S. drilling project called GISP2 (*Greenland Ice Sheet Project II*) was aiming at similar drilling objectives just circa 30 km west of Summit. Collaboration on the field between the two drilling parties was very good and helped to save costs for both projects. In 1992 the GRIP ice-coring team reached bedrock at 3029 m depth. Approximately one year later a 3053 m deep ice core was recovered to bedrock depth at the GISP2 site.

These two sibling cores provided a wealth of information about the climate history of the North-Atlantic region in the last 115 ka. In particular, they revealed a remarkably turbulent climate during the last glacial period (14–114 ka BP), characterized by what became known as *Dansgaard–Oeschger events*: rapid climate fluctuations at intervals ranging from few hundred to few thousand years (Dansgaard et al. 1993). Such abrupt changes could be identified not only in other Greenland cores (e.g. Camp Century, Dye-3) but also in marine sediment records of the North Atlantic, which indicate large-scale shifts in ocean currents (Bond et al. 1993; Johnsen et al. 1992). In contrast, the identification of similar events in Antarctica was hampered by the generally lower snow accumulation, which increases the chance of finding older climate records, but reduces their chronological resolution.

Actually, the situation was such that, by the end of the GRIP–GISP2 drilling projects, there was only one Antarctic ice core extending through the last glacial period and beyond: the *Vostok Deep Ice Core*, extracted at the homonymous Soviet research station, which was established in 1957 during the IGY (Fig. 2.8). The Vostok core revealed a close connection between climate and the atmospheric concentration of greenhouse gases back to 420 ka BP (Jouzel et al. 1993; Petit et al. 1999), but it showed no clear evidence of an Antarctic counterpart to Dansgaard–Oeschger events (Paterson 1994).

Fig. 2.8 Location of some deep ice-coring sites in Antarctica.
 ① Byrd, ② Siple Dome,
 ③ Taylor Dome, ④ Law Dome,
 ⑤ EPICA Dome C,
 ⑥ Vostok, ⑦ Dome Fuji,
 ⑧ EPICA-DML. After
 Steinhage (2001). Courtesy of
 D. Steinhage (AWI)



These results made patent that high-resolution records from Antarctica's South-Atlantic sector were necessary to complement the records obtained in central Greenland. On the other hand, there was also the lasting desire to go further back in time with ever older ice cores. It was in this spirit that the Antarctic counterpart to GRIP, called the *European Project for Ice Coring in Antarctica* (EPICA) came out in the early 1990s. EPICA was conceived as a multinational inter-European consortium with the objective of drilling two ice cores to bedrock on the East-Antarctic Plateau within a decade. At *Dome C*, in the Indian Sector, the target was old ice, with the largest possible amount of glacial–interglacial cycles in one record. At *Dronning Maud Land* (DML), in the Atlantic Sector, the aim was to obtain a South-Atlantic counterpart to the high-resolution Greenland records, covering at least one complete climate cycle (Fig. 2.8).

2.5 EPICA Facts and Figures

The European Project for Ice Coring in Antarctica (EPICA) was organized in a threefold funding scheme:

1. as two successive programmes of the European Science Foundation (ESF);
2. as 3 + 1 projects within successive Framework Programmes of the European Commission (EC);
3. as a number of national contributions from the ten European nations formally involved in EPICA: Belgium, Denmark, France, Germany, Italy, the Netherlands, Norway, Sweden, Switzerland, and the United Kingdom.

EPICA started as a five-year ESF Research Programme in January 1996, which was then extended for further five years in 2001, and eventually continued for one extra year until the end of 2006. During this eleven-year period ESF contributed a total of EUR 490,000 to the Programme (Oerter et al. 2009), which were made available mainly for coordination, meetings, and publications. The EPICA Programme was managed by a Scientific Steering Committee chaired from 1996 to 2001 by Jean Jouzel (Climate and Environment Sciences Laboratory, LSCE, Saclay), and subsequently by Heinz Miller (Alfred Wegener Institute, AWI, Bremerhaven) until 2006.

Table 2.1 The EPICA–EC grants (after Oerter et al. 2009)

| Project | Reference [†] | Duration | Grant [‡] |
|-----------|------------------------|-------------------|--------------------|
| EPICA 1 | ENV4-CT95-0074 | Feb 1996–Jan 1999 | 5.0 |
| EPICA 2 | ENV4-CT98-0702 | Feb 1999–Apr 2001 | 2.9 |
| EPICA 3 | EVK2-CT-2000-00077 | May 2001–Apr 2004 | 2.4 |
| EPICA-MIS | STREP-003868 | Dec 2004–May 2008 | 2.5 |

[†]Sometimes the dashes and/or the letters “CT” are omitted

[‡]Million EUR

Table 2.2 Summary data on the two EPICA drilling sites

| | Dome C [†] | Dronning maud land [‡] |
|---------------------------------|--|--|
| Ice-core notation | EDC96 and EDC99 | EDML |
| Station name | Concordia | Kohnen |
| Location | 75°06′04″S, 123°20′52″E | 75°00′06″S, 00°04′04″E |
| Elevation (a.s.l.) | 3233 m | 2892 m |
| Ice thickness | 3309±22 m | 2782±10 m |
| Ice-core length | 3259.72 m | 2774.15 m |
| Ice-core age | ca. 800,000 years | ca. 150,000 years (at 2416 m) possibly 250,000 years (near bedrock) |
| Accumulation rate (annual mean) | 25.0 kg m ⁻² a ⁻¹ (present time scale) 25.6 kg m ⁻² a ⁻¹ (using Tambora) 25.4 kg m ⁻² a ⁻¹ (last 1000 years) | 64.0±0.5 kg m ⁻² a ⁻¹ (last 1000 and 4000 years) 65 kg m ⁻² a ⁻¹ (from radar) |

[†] <http://www.esf.org> (retrieved on 30 Nov 2015, search word: EPICA)

[‡] Ibid. and Oerter et al. (2009)

Field work of EPICA was co-funded by three subsequent EC grants within the 4th–6th European Framework Programmes (Table 2.1), as well as one Specific Targeted Research Project, called EPICA-MIS (Enhanced Paleo-reconstruction and Integrated Climate Analysis through Marine and Ice-core Studies). According to Wilhelm et al. (2014), the EC grants amounted to circa 25% of the total budget, while multiple national contributions (which are difficult to estimate precisely) covered the remaining 75%.

The main logistic support for Dome C was provided by Italy and France through PNRA (National Research programme in Antarctica) and IPEV (Institute Paul Emile Victor), respectively. On the other hand, Germany (AWI) was in charge of the logistics for Dronning Maud Land.

Scientific activities were planned and coordinated by a Scientific Committee led by Bernhard Stauffer (University of Bern) in the period 1996–2002, and then by Eric Wolff (British Antarctic Survey, BAS, Cambridge) until 2006. Research was arranged in five basic consortia: isotopes, gases, chemistry, dust, and ice physical properties. Smaller teams dealt with ice sheet modelling and meteorology, while two special groups were formed during the course of the project for dating and biological studies.

The EPICA science plan, formulated in 1994, addressed many of the major paleoclimate issues of the time, especially that of investigating past climate cycles (with an expected time coverage of 500,000 years, much less than was eventually achieved), and of understanding the geographical and

temporal scope of rapid climate changes during glacial periods. To achieve these goals EPICA used drill rigs heavily based on designs previously developed by Danish scientists and colleagues for Greenland deep-drilling programmes (cf. Sects. 3.2 and 3.3).

At *Dome C* (75°06′S, 123°21′E, also known as EDC; cf. Table 2.2), next to the all-year French–Italian Concordia Station, drilling started in 1996, but the drill got stuck at 788 m depth and the borehole was abandoned in 1999 (EPICA Community Members 2004). This first core became known as EDC96. Drilling of the second core (EDC99, sometimes also called EDC2) started in 1999, circa 10 m apart from the EDC96 borehole, and stopped at a logged depth³ of 3259.72 m in December 2004, nearly 15 m above bedrock (Jouzel et al. 2007), after seismic soundings suggested the presence of melt water just below. Ice at the bottom of the EDC99 core is estimated to be older than 800 kaBP (Jouzel et al. 2007; Parrenin et al. 2007).

In *Dronning Maud Land* (DML), an extensive pre-site survey (Steinhage 2001) led to a drilling site at 75°00′S, 00°04′E, now known as Kohnen Station (Table 2.2). Deep drilling started in January 2002 and finished in January 2006 at a logged depth of 2774.15 m, nearly 10 m above bedrock, after subglacial water poured into the borehole (Oerter et al. 2009). Dating of the core could be performed unambiguously down to 2416 m depth, corresponding to circa 150 kaBP (Ruth

³For a definition of *logged depth*, see the Glossary in Sect. 1.2.

et al. 2007). For the remaining 358 m of the core (approximately 13% of the core length, possibly corresponding to further 100,000 years) the core could not be dated, because of flow disturbances that corrupted the stratigraphy (Faria et al. 2010, 2014b; Ruth et al. 2007, see Chap. 4). Thus, the paleoclimate records of the EPICA-DML Deep Ice Core (usually called EDML) cover a complete glacial cycle in relatively high resolution, and serve as a direct southern-hemisphere counterpart to the Greenland records (e.g. GRIP, GISP2, and the more recent NorthGRIP and NEEM ice-core records; EPICA community members 2006).

These findings and many others have been highlighted in more than 300 scientific publications to date, including

two EPICA community papers (EPICA Community Members 2004; EPICA community members 2006) and a special EPICA issue (Barbante et al. 2010). EPICA data have featured heavily in authoritative assessment reports, such as those of SCAR (Scientific Committee on Antarctic Research), or the 4th and 5th Assessment Reports of IPCC (Intergovernmental Panel on Climate Change). The achievements of EPICA were also recognized by the Descartes Prize for Excellence in Scientific Collaborative Research 2007, awarded to EPICA by the European Commission. Likewise, several EPICA scientists have been honoured with awards from respected bodies like the European Geophysical Union (EGU) and others.

The EPICA-DML Deep Ice Core

A Visual Record

Faria, S.H.; Kipfstuhl, S.; Lambrecht, A.

2018, XI, 305 p. 39 illus., 31 illus. in color., Hardcover

ISBN: 978-3-662-55306-0